Hydrodenitrogenation of 1, 2, 3, 4-Tetrahydroquinoline Over CoMoS/Mesostructured TiO 2 Catalysts

Sylvette Brunet, Teddy Roy, Bénédicte Lebeau, Laure Michelin, Jean-luc Blin

▶ **To cite this version:**

Sylvette Brunet, Teddy Roy, Bénédicte Lebeau, Laure Michelin, Jean-luc Blin. Hydrodenitrogenation of 1, 2, 3, 4-Tetrahydroquinoline Over CoMoS/Mesostructured TiO 2 Catalysts. Energy Technology, 2024, 12 (7), pp.2400321. 10.1002/ente.202400321 . hal-04659051

HAL Id: hal-04659051
https://hal.science/hal-04659051

Submitted on 22 Jul 2024

HAL is a multi-disciplinary open access archive for the deposit and dissemination of scientific research documents, whether they are published or not. The documents may come from teaching and research institutions in France or abroad, or from public or private research centers.

L'archive ouverte pluridisciplinaire **HAL**, est destinée au dépôt et à la diffusion de documents scientifiques de niveau recherche, publiés ou non, émanant des établissements d'enseignement et de recherche français ou étrangers, des laboratoires publics ou privés.

Distributed under a Creative Commons Attribution 4.0 International License

Hydrodenitrogenation of 1, 2, 3, 4-tetrahydroquinoline over CoMoS/mesostructured TiO_2 catalysts

Sylvette Brunet[1*], Teddy Roy[1], Benedicte Lebeau[2,3], Laure Michelin[2,3], Jean-Luc Blin[4*]

[1] : Université de Poitiers, CNRS, IC2MP, UMR 7285, 86073 Poitiers Cedex 9 France.
[2] : Université de Haute Alsace (UHA), CNRS, IS2M UMR 7361, F-68100 Mulhouse, France
[3] : Université de Strasbourg, F-67000 Strasbourg, France
[4]: Université de Lorraine, CNRS, L2CM, F-54000 Nancy, France

Corresponding authors : jean-luc.blin@univ-lorraine.fr; sylvette.brunet@univ-poitiers.fr

Table of Contents

Mesostructured titania-based catalysts promote the hydrodenitrogenation of 1,2,3,4-tetrahydroquinoline, enhancing both the hydrogenation and the C-N bond cleavage. The catalytic performance is correlated to the mesopore diameters.

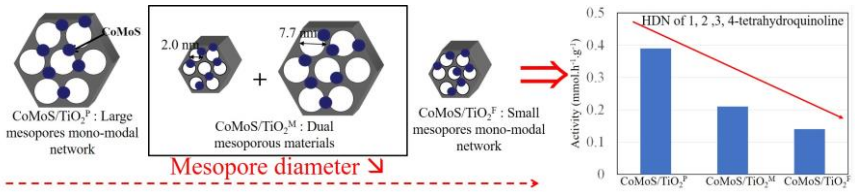

Abstract
Here, we report the design of new catalysts obtained by the dispersion of the CoMoS active phase on mesostructured titania having different pore size and kind of porosity (monomodal vs dual) for hydrodenitrogenation (HDN) of 1, 2, 3, 4-tetrahydroquinoline (1234THQ). Obtained results show that with a selectivity around 93%, the hydrogenated pathway is by far the main route for 1234THQ hydrodenitrogenation. We also demonstrate that the catalytic activities depend on the mesopore diameter: the larger the size of the mesopores is, the higher the HDN activity is. Comparing with the conventional $CoMoP/Al_2O_3$ catalyst, a slightly higher activity is obtained for the mesostructured TiO_2-based catalyst due to the promoter effect of titania.

Keywords: Heterogeneous catalysis; Hydrodenitrogenation; Mesoporous materials; Titania

1. Introduction

Air pollution is one of the major challenges facing our society. Gases that are toxic to humans and pollute the atmosphere mainly come from the transport sector. Nitrogen oxides (NOx) and sulfur oxides (SOx) are the majority representatives. In order to limit their impacts on the environment and on human health, it is thus necessary to reduce emissions linked to transport [1-4]. To improve this goal, it is necessary to intensify processes to make them more eco-efficient in order to produce clean fuels (10 ppm of sulfur since 2009) which requires the development of more powerful hydrotreating catalysts.

Hydrotreating combines catalytic operations in which, at high temperature and under hydrogen pressure, the impurities present in the petroleum fractions (sulfur, nitrogen or metal-containing molecules) are eliminated and certain unsaturated molecules are hydrogenated [5]. Among the hydrotreating processes, hydrodesulfurization (HDS) and hydrodenitrogenation (HDN), which makes possible to reduce the sulfur and nitrogen content, respectively, of petroleum feedstock (mainly gazole) are of peculiar interest in regard to the negative effects of SOx and NOx on air quality. As reported in the literature for several decades, the main refractory sulfur and nitrogen compounds are represented by alkylbenzothiophenes for the sulfur compounds [6] and acridine, quinoline for the nitrogen compounds [7-9] which involved the main two reactions in hydrotreatments i.e hydrogenation and C-S or C-N bond rupture. 4,6-dimethydibenzothiophene (46DMDBT) and of 1, 2 ,3, 4-tetrahydroquinoline (1234-THQ), are model molecules representative of those contained in the crude.

Conventional hydrotreating catalysts are based on transition metal sulfides (MoS_2, WS_2) usually promoted by nickel or cobalt leading to NiMoS or CoMoS active phase mainly supported over alumina [10]. Indeed, this support is well known to well disperse the active phase and also for its good mechanical properties during the shaping of the catalysts for their use at the industrial scale. However, γ-Al_2O_3 has also some drawbacks such as a strong Lewis acidity and strong metal-support interactions that can have a negative effect on the activity of the hydrotreating catalysts [11]. Moreover, the interactions of the support with Mo will modify the electronic properties of the coordinately unsaturated sites (CUS) of molybdenum, which are known to be the active sites of MoS_2 [10].

The following properties are desirable for the development of a good hydrotreating catalyst support: adequate textural properties [12], high activity and selectivity [13], appropriate acidity [14] and optimal metal support interaction [15]. In particular, good textural properties are considered to be one of the most important criteria that any hydrotreating catalyst support should fulfill for the hydrotreating of heavy feeds [12, 16]. Adequate catalyst support's textural properties, namely high specific surface area, well-ordered uniform pore structure containing mesopores stable to thermal treatments, and narrow pore size distribution, facilitates the dispersion of active components on it and helps to maximize the utilization of

the active component in the pores [17-18]. Moreover, adequate porosity is required to increase the catalyst life time since the life within a smaller pore size catalyst can be reduce due to cocking and pore mouth plugging [13].
Among the various support such as amorphous aluminosilicate, alumina, carbon materials, molecular sieves, titania is a promising support for hydrotreating processes due to its higher capacity to interact with molybdenum. For example, Wang et al. [19] in a paper dealing with the use of TiO_2-containing bulk Ni_2P as catalyst for HDN of quinoline and decahydroquinoline have shown that the introduction of titania improves both the hydrogenation and the C-N bond cleavage activities of Ni_2P. The support plays therefore an important role in improving the properties of a catalyst in terms of activity, selectivity, and stability, by manipulating its surface properties [17, 20]. In this respect,
As explained above, due to its higher capacity to interact with molybdenum, TiO_2 is particularly intriguing as support for hydrotreating [21-24]. But for reasons, which are now well understood, the advantage of TiO_2 over Al_2O_3 is largely lost when we deal with Co- or Ni-promoted catalysts [25]. Another handicap of TiO_2 supports is that they often have low specific surface areas and pore volumes [26], which makes it impossible to achieve high Mo loadings and hence limits the activity. Thanks to their properties such as high specific surface area, narrow pore size distribution, mesostructured metal oxides are excellent candidates to meet the criterion required for an efficient hydrotreating catalyst support. In particular mesostructured TiO_2 can overcome the drawbacks generally encountered when titania is used as support for hydrotreating process. These materials can be prepared according to various pathways [27]. Among them, the evaporation –induced self-assembly (EISA) route is one of the most synthetic methods in the research area of surfactant-assisted mesoporous materials [25,28]. Combining the EISA pathway, usually used for the preparation of the mesoporous films, and the liquid crystal templating mechanism, we have prepared mesostructured titania with 2D hexagonal porous network, having semi-crystalline framework and with high specific surface area (> 250 m^2/g) [29,30]. Pluronic P123, an amphiphilic triblock copolymer, is used as pore templating agent and titanium isopropoxide as inorganic precursor. The mesostructure is stable until 500°C [30]. These mesostructured TiO_2 having a part of amorphous phase have also been used for the preparation of Co-promoted MoS_2 hydrotreatment catalysts, which were successfully tested in the conversion of 4,6-dimethydibenzothiophene (46DMDBT) [31,32]. Here, the designed CoMoS/mesostructured TiO_2 catalysts have been evaluated for the HDN of 1, 2 ,3, 4-tetrahydroquinoline (1234THQ), used as a model molecule representative of those present in gazole cut. We have investigated in particular the effect of the mesopore size on the HDN activity. Results have also been compared with the ones obtained from a $CoMoP/Al_2O_3$ commercial catalysts and from two commercial TiO_2 supports M311 and M411. These supports have been impregnated and sulfided under the same conditions used for the mesostructured TiO_2.

2. Materials and methods

Cobalt(II) nitrate hexahydrate ($CoN_2O_6.6H_2O$, 99.00 % Sigma-Aldrich) and ammonium heptamolybdate [$(NH_4)_6Mo_7.6H_2O$, 99.98 % Sigma-Aldrich] were used as Co and Mo precursors, respectively. M411 and M311 supports have been provide by Hunstman. M311 is a pure titania support and M411 contains 7 wt% of SiO_2.
The $CoMoP/Al_2O_3$ catalyst is a commercial one with the following composition: 15.4 wt% of MoO_3, 4.3 wt% of CoO and 1.6 wt% of phosphorus and a specific surface area of 216 m^2/g.

2.1. Catalyst preparation.

The catalysts have been obtained by wet impregnation of the support according to the method reported in reference 32. The targeted number of Mo atoms per nm^2 and the Co/Mo ratio were

fixed to 3 and 0.54, respectively. The precursors were then decomposed at 380°C under air during 5 hours. The mesostructured TiO_2 supports have been prepared from $C_8F_{17}C_2H_4(OC_2H_4)_9OH$ [$R^F_8(EO)_9$], triblock copolymer P123 $(EO)_{20}(PO)_{70}(EO)_{20}$ (EO = ethylene oxide, PO = propylene oxide) and a mixture containing 50 wt% of each surfactant via the sol-gel method. The obtained supports are labelled as TiO_2^F, TiO_2^P and TiO_2^M, respectively. By this way we were able to vary the porosity [33].

2.3. Characterization

Bare, impregnated supports and catalysts obtained after sulfidation have been characterized by Small Angle X-ray Scattering (SAXS), nitrogen adsorption desorption analysis, Raman spectroscopy, XRD, TEM and XPS according to procedures described elsewhere [32]. N_2 adsorption-desorption isotherms were determined on a Micromeritics TRISTAR 3000 sorptometer at –196 °C. The specific surface area was obtained by using the BET model whereas the pore diameter and the pore size distribution were determined by the BJH (Barret, Joyner, Halenda) method applied to the adsorption branch. The measurement of the acidity by adsorption of pyridine followed by FTIR spectroscopy was carried out with a ThermoNicolet NEXUS 5700 spectrometer at a resolution of 2 cm^{-1} and collected 128 scans per spectrum. Catalyst samples were pressed into thin pellets (10-60 mg) with diameter of 16 mm under a pressure of 1-2 $t.cm^{-2}$ and activated in situ during one night under nitrogen at 380°C. After cooling down the samples until room temperature, a background spectrum was collected. The quantity of Lewis and Brönsted acid sites was determined from the area of the band at 1445-1450 cm^{-1} for the Lewis acidity and at 1540 cm^{-1} for the Brönsted acidity [34,35]. All spectra were normalized to an equivalent sample mass (20 mg) to compare them against each other. Detailed results have been reported in reference 32.

2.3. Sulfidation and catalytic measurements:

As reported in previous papers [32, 36], the catalysts are sulfided in situ in a fixed flow reactor using a sulfiding feed made of 5.8 wt% of dimethyl disulfide (DMDS) in n-heptane as solvent at a temperature of 350 °C under a 4.0 MPa of total pressure during 14 h. The temperature was then lowered to the reaction temperature (340 °C).

Then, HDN of 1234THQ was carried out at 340°C and 4.0 MPa of total pressure after the in situ sulfidation of the catalyst according to the procedure described above. The feed was composed by 1234THQ (1.55 wt%) diluted in n-heptane into which dimethyl disulfide (1.27 wt%) was added to generate H_2S. The ratio H_2/feed was fixed to 475 NL/L.

The transformation of 1234THQ was analyzed with a Varian 3400 chromatograph equipped with a 25 m BP1 (SGE) capillary column (inside diameter: 0.32 mm; film thickness : 5 μm) with a temperature program from 50 to 70°C (4°C/min) then from 70 to 250°C (15°C/min). For this, the liquid sample of the reaction was collected each hour and then injected manually in the gas phase chromatograph.

All products were identified by GC-MS (Finnigan INCOS 500) and by comparison with commercial products.

The reaction scheme of transformation of 1234THQ (Scheme 1) is well known [37]. Three main families of products were identified i.e. hydrogenation-dehydrogenation products (quinoline, 5,6,7,8 tetrahydroquinoline: 5678THQ, decahydroquinoline: DHQ); HDN products (propylcyclohexane: PCH and propylbenzene: PB) and DDN (Direct DeNitrogenation) products (only orthopropylaniline).

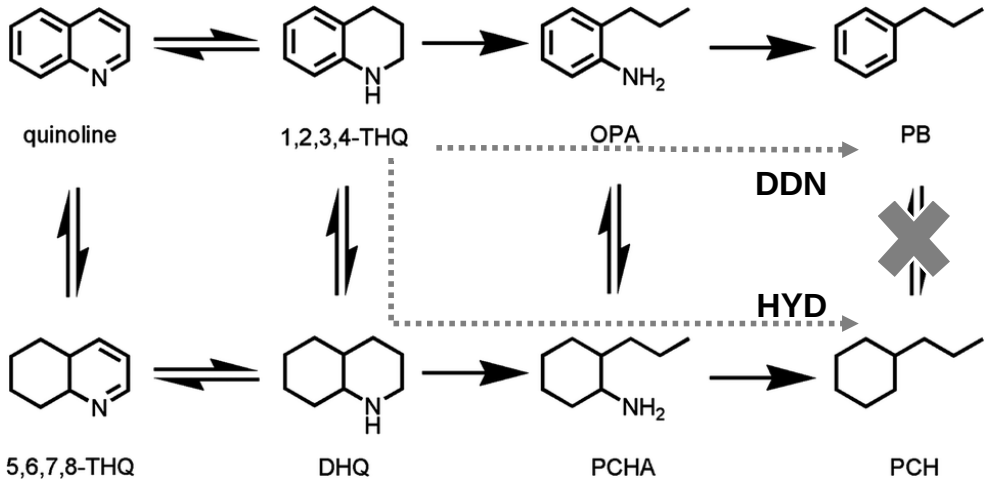

DDN : Direct denitrogenation, formation of propylbenzene
HYD : Hydrogenation of the aromatic ring before breaking the C-N bond

Scheme 1 : Pathways for 1, 2 ,3, 4-tetrahydroquinoline transformation.

The total catalytic activity (A_{total}) was calculated at isoconversion (25%) in a differential regime according to the following equation:

$$A = \ln\left(\frac{1}{1-X_i}\right).\frac{F}{m_{cat}}$$

where F is the molar flow of the reactant in mmol/h, m_{cat} is the mass of catalyst in g and X is the 1234THQ conversion. Conversions of 1234THQ were collected after the stabilization. Different activities (A) were considered and they are defined as follow. The total activity is calculated from the conversion of 1234THQ. A_{HDN} is related to the activity for HDN of 1234THQ corresponding to the formation of the total denitrogenation products i.e. orthopropylbenzene (OPA) and propycyclohexane (PCH) (Scheme 1). A_{HYD} means the activity for the hydrogenation route corresponding only to the formation of the PCH resulting to the hydrogenation step followed to C-N bond rupture. A_{DDN} corresponds to the activity of the formation only of orthopropylaniline (OPA) resulting only of the C-N bond rupture. The selectivity (%) towards HYD and DDN were calculated respectively by the ratio between $A_{HYD}/(A_{HYD+}A_{DDN})$ and by $A_{DDN}/(A_{HYD+}A_{DDN})$.

3. Results and discussion:

3.1. Properties of the impregnated CoMo/TiO_2 catalysts

As expected, the good metal contents (Mo and Co) were well impregnated whatever the support (Table 1).

Table 1 : Composition determined by X-ray fluorescence, variation of the specific surface area (S_{BET}), the pore volume (Vp), the mesopore diameter (∅), Lewis (L) and Brönsted (B) acidity measurement by FTIR pyridine of the various TiO_2 support after wet impregnation.

		TiO_2^F	TiO_2^P	TiO_2^M	M311	M411
MoO_3 (wt %)		15.7	14.2	14.6	15.4	14.2
CoO (wt %)		4.4	4.0	4.1	4.3	4.0
S_{BET} (m^2/g)		220	200	205	216	200
Vp (cm^3/g)		0.13	0.30	0.18	0.36	0.36
∅ (nm)		2.0	6.6	2.0/7.7	-	-
n_{pyr} ($\mu mol\ g^{-1}$)	L	294	331	264	368	345
	B	97	85	82	50	71
B/L		0.33	0.26	0.31	0.14	0.20

Impregnated mesostructured TiO_2 have a hexagonal mesopore network with nanosized anatase semi-crystalline framework [33]. By contrast no reflection line is detected on the SAXS pattern of M311 and M411 (Fig 1A). These materials do not present any mesopore ordering. As observed on the Raman spectra (Fig. 1B) and on the SEM images (Fig. 1C), they are mainly constituted of spherical anatase particles. Indeed, the vibrations observed at 150, 396, 515 and 639 cm^{-1} on the Raman spectra can be assigned to the E_g, B_{1g}, A_{1g}+B_{1g} and E_g modes of anatase [38].

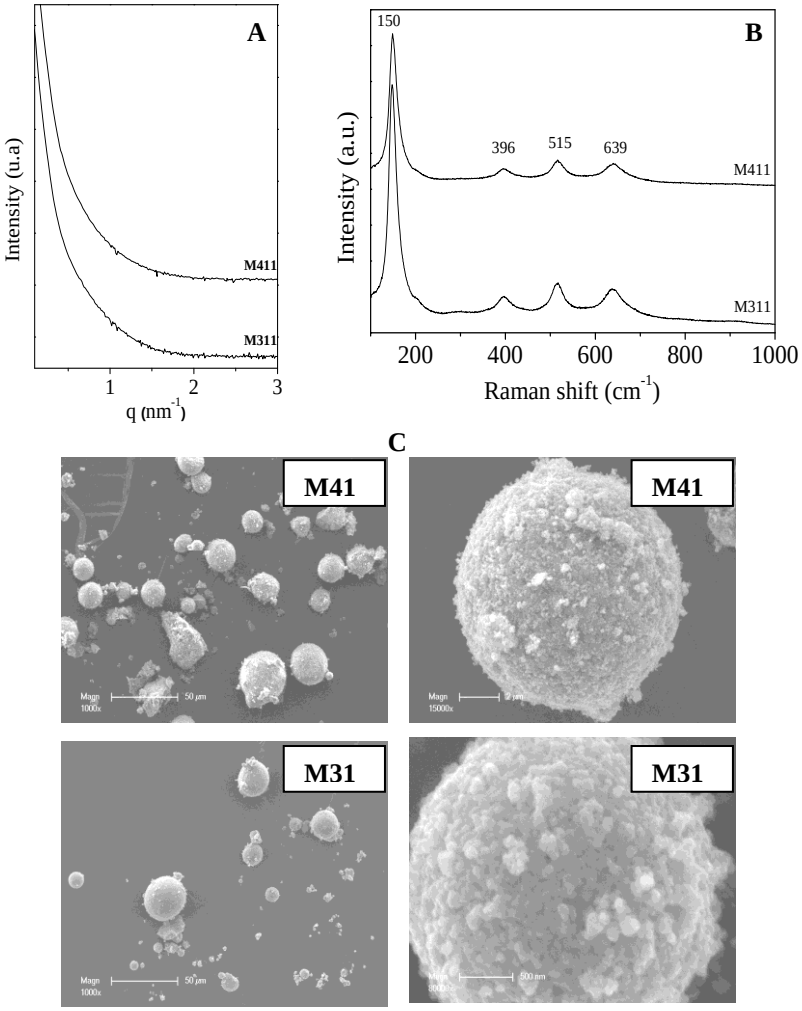

Figure 1 : SAXS (A) pattern, Raman spectrum (B) and SEM (C) images of M311 and M411.

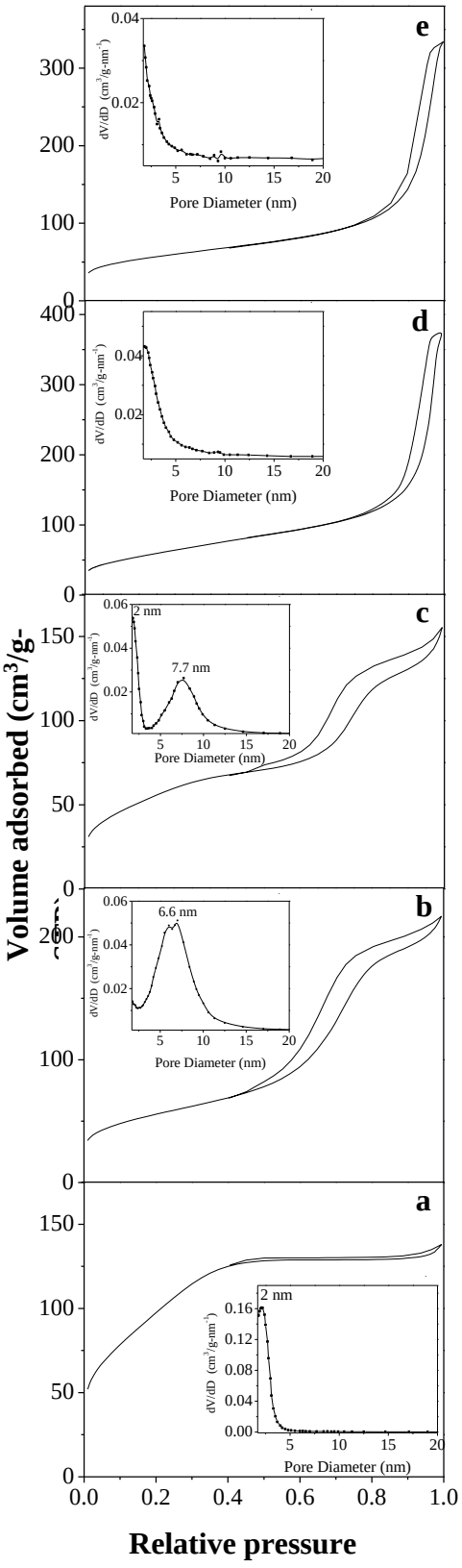

Figure 2 : Nitrogen adsorption-desorption isotherms and pore size distributions (insert) of the support after wet impregnation. Supports are TiO_2^F (a); TiO_2^P (b), TiO_2^M (c); commercial TiO_2 M311 (d) and M411 (e).

According to the IUPAC classification [39], the impregnated mesostructured TiO_2 exhibit type IV nitrogen adsorption-desorption isotherm (Fig. 2), characteristic of mesoporous materials. For TiO_2^M two inflection points are observed on the isotherm, this reflects the presence of mesopores with two different sizes. The mesopore size distributions obtained from the BJH method applied to the adsorption branch of the isotherm (insert of Fig. 2), confirm the presence of an intrinsic mesoporosity and the formation of a dual mesopore network for the titania support obtained from the porogen agents mixture. The pore size distribution is centered around 2.0, 6.6 and 2.0/7.7 nm for the supports prepared from $R^F_8(EO)_9$, P123 and a 50 wt% $R^F_8(EO)_9$/P123 mixture, respectively. The mesopore diameter of the supports can be related to the size of the cylinders of the hexagonal phase, which has been used as template for their preparation [33].

For the two commercial titania materials, the situation is quite different. Indeed, the isotherm is rather type II and no maximum is detected in the mesopores range (Fig. 2), meaning that there is no intrinsic mesoporosity. Whatever the impregnated support the specific surface area is around 200 m²/g (Table 1). The pore volume varies from 0.13 to 0.30 cm^3/g for the mesostructured supports and it is equal to 0.36 cm^3/g for the two commercial TiO_2. For these samples, the porosity is thus interparticular. The condensation of nitrogen occurs between the spherical particles observed by SEM. The pyridine adsorption followed by FTIR [34,35] has been used to characterize the acidity properties of the titania materials (Table 1). All impregnated TiO_2 have a significant acidity, and in particular a Brønsted one. They all present a Lewis acidity in the same range of order, between 294 and 345 µmol g^{-1}. In addition to the Lewis acidity, a Brønsted acidity, around 85-90 µmol.g^{-1} is observed for the mesostructured supports. The value of the latter is slightly lower for M311 (50 µmol.g^{-1}) and M411 (71 µmol.g^{-1}). According to literature, the Lewis acidity can be attributed to the presence of the anatase phase. Indeed, Afanasiev et al. have shown that strong Lewis acid sites are present on anatase and rutile surface [40]. By contrast the Brønsted acidity can be linked to the hydroxyl group present at the surface of the amorphous phase, which coexists with anatase. Indeed, when heated at temperature ranging from 450°C to 650°C, the crystallization of the wall of the mesostructured

titania is increased and meantime the Brønsted acidity strongly decreases [41].
The complete characterization of the sulfided phases dispersed on the mesostructured titania has been reported in detail in reference 32. After sulfidation, the length of the MoS_2 slabs is found between 1.5 and 6.0 nm. From XPS data, the sulfidation rate of molybdenum (TSMo), global sulfidation degree (TSG), promotion rate (PR), atomic S/Mo and Co/Mo ratios are found to be equal to 53%, 69%, 36%, 1.8 and 0.3, respectively [32]. Whatever the support, these values are similar [32].

3.2. HDN of 1, 2 ,3, 4-tetrahydroquinoline

The catalysts were rapidly stable after four hours of reaction time corresponding to the setting of the system.

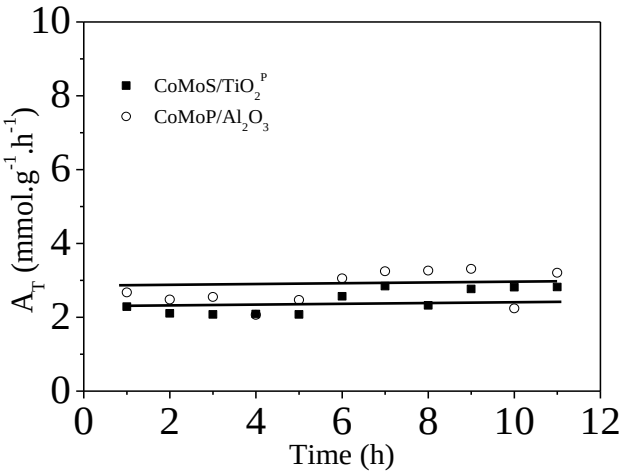

Figure 3 : Transformation of the 1, 2 ,3, 4-tetrahydroquinoline. Total activity of the $CoMoS/TiO_2^P$ and $CoMoP/Al_2O_3$ catalysts as a function of the reaction time. (T=340°C, P=4.0 MPa, H_2/feed=475 Nl/l).

Indeed, as depicted in Figure 3 for the $CoMoS/TiO_2^P$ catalyst, given as example, as a function of reaction time, the activity is almost constant. For $CoMoS/TiO_2^P$, reported as example, the conversion of 1234THQ increases with the contact time (Fig. 4).

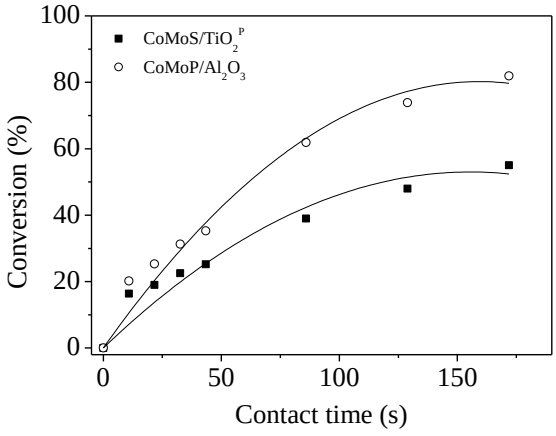

Figure 4 : Transformation of the 1, 2 ,3, 4-tetrahydroquinoline. Conversion as a function of the contact time. Comparison of $CoMoS/TiO_2^P$ and $CoMoP/Al_2O_3$ (T=340°C, P=4.0 MPa, H_2/feed=475Nl/l).

Its value is changed from 17 to 50% when the contact time is varied from 10.9 to 130 s and a plateau is reached at 50%. The same trend is obtained with the $CoMoP/Al_2O_3$ conventional catalyst. However, for a given contact time the latter leads to a higher conversion rate of 1234THQ and the plateau is obtained at around 80%. For example, if the contact time is equal to 25s, a conversion of 28% is obtained using the conventional catalyst against 12% for the mesostructured TiO_2-based catalyst.
The representative product distributions from 1234THQ transformation over CoMoS/mesostructured titania catalysts (whatever the properties of TiO_2) is the same and depicted in Figure 5 for $CoMoS/TiO_2^P$ as example.

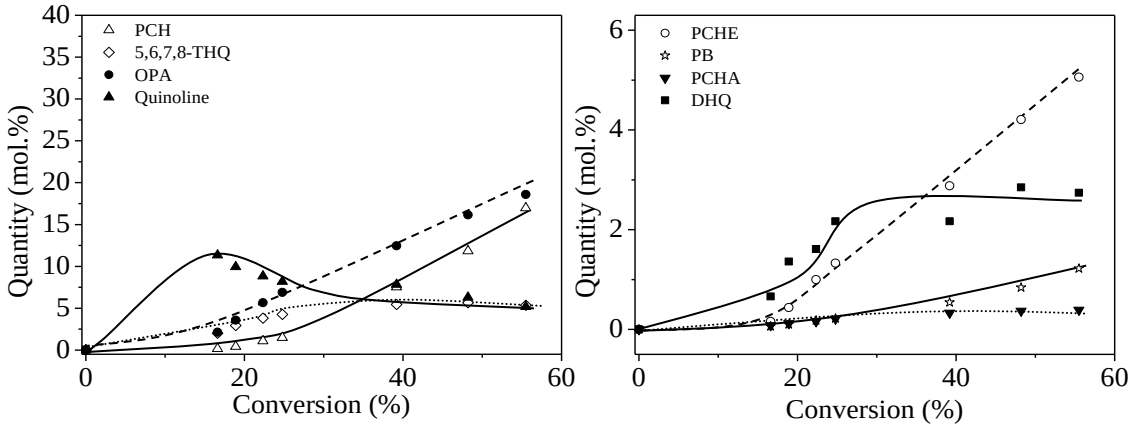

Figure 5 : Transformation of 1, 2 ,3, 4-tetrahydroquinoline. Distribution of products as a function of the conversion. (T=340°C, P=4.0 MPa, H_2/feed=475 Nl/l, CoMoS/mesostructured TiO_2^P).

Until a conversion value around 20%, the amount of quinoline increases up to 11% then its value slightly decreases to reach 5 mol.% at 55.5% of conversion. The presence of quinoline, 5678THQ, DHQ can be explained by the various equilibrium involving hydro-dehydrogenation reactions. Moreover, it is well known that when starting from quinoline its hydrogenation to give 1234THQ (Scheme 1) is very fast and an equilibrium is reached at all reaction conditions [42,43] an act as 1234THQ substrate. The formation of o-propylaniline (OPA), propylcyclohexane (PCH), decahydroquinoline (DHQ), propylcyclohexylamine (PCHA), probylbenzene (PB) and propylcyclohexene (PCHE) is also observed. It should be noted that PCHE is a reaction intermediate, which is converted into PCH [43]. For the $CoMoS/TiO_2^P$ catalyst, as a function of the conversion the proportion of both OPA and PCH continuously increases from 0 to 18.6 and from 0 to 17.0, respectively. The quantity of PB is rather low. Its increases from 0 to 1.2 mol% when the conversion is varied from 0 to 55.5 %. Similarly, DHQ, PCHE, 5678THQ and PCHA are observed in a low proportion. Indeed, the amount of PCHA and PCHE are respectively around 0.4 and 5 mol% for a conversion of 55.5 %. The ones of DHQ and 5678THQ increase respectively from 0 to 2.2 mol% and from 0 to 5.5 mol%, when the conversion varies from 0 to 39 % and then they remain almost constant. The product distributions are similar to the ones obtained when the conventional $CoMoP/Al_2O_3$ catalyst is used instead of the titania ones (Fig. 6).

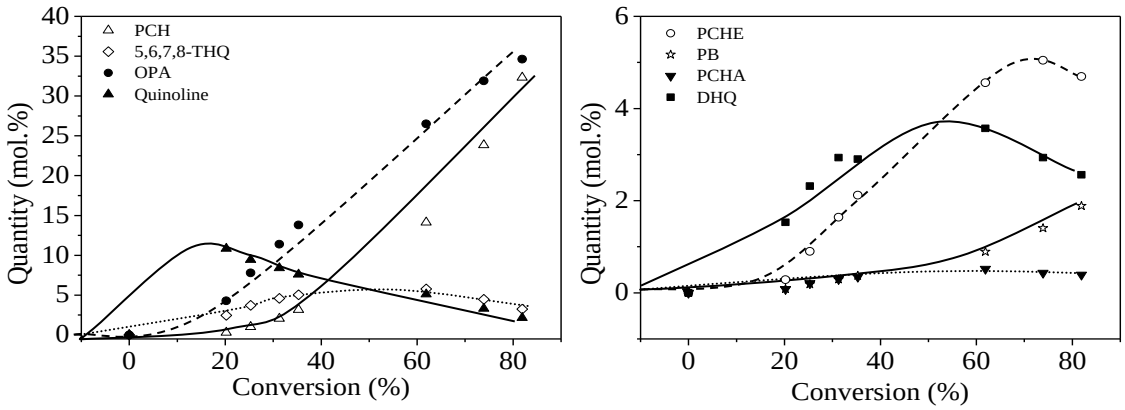

Figure 6 : Transformation of 1, 2 ,3, 4-tetrahydroquinoline. Distribution of products of as a function of the conversion. (T=340°C, P=4.0 MPa, H_2/feed=475 Nl/l, $CoMoP/Al_2O_3$)

From the product distributions, it can be concluded that whatever the considered catalyst, PCH is the major nitrogen free product obtained, indicating that HYD is the main route for the transformation of 1234THQ. PB has been detected in low quantity even if OPA is observed in a larger amount. The presence of OPA in this proportion can be related to the fact that its decomposition is almost completely inhibited by the presence of other products such as quinoline [37,44]. The facile conversion of DHQ to PCHA is in good accordance with its low amount (≈ 2.2 mol% or a conversion of 39 %). Since PCHA transforms as quickly as it forms [43], it is detected in a negligible quantity (≈ 0.4 mol%). In addition, the Hofmann-type elimination of PCHA to PCHE is rather rapid. It should be also outlined that under the catalytic conditions and the type of catalysts used in this study the hydrogenation of PB to give PCH cannot take place [45].
The performance of the different TiO_2 properties as support of CoMoS catalysts have been compared in terms of activities (A_{total}, A_{HDN}) and the selectivities (HYD and DDS) for the transformation of 1234THQ involving a hydrogenation way (HYD) in one hand and the direct DDN way in other hand. (Table 2).

T**able 2** : Transformation of 1234THQ. Activities (A $mmol.h^{-1}.g^{-1}$) and selectivity (HYD, DDN) (%) of the various catalysts (T=340°C, P=4.0 MPa, H_2/feed=475 Nl/l, 25% conversion)

	Activity ($mmol.h^{-1}.g^{-1}$)		Selectivity (%)	
Catalyst	A_{total}	A_{HDN}	HYD	DDN
$CoMoS/TiO_2^P$	3.1	0.39	92	8
$CoMoS/TiO_2^M$	2.1	0.21	93	7
$CoMoS/TiO_2^F$	1.5	0.14	93	7
CoMoS/M311	2.4	0.28	95	5
CoMo/M411	2.4	0.34	93	7
$CoMoSP/Al_2O_3$	4.0	0.30	88	12

TiO_2^P : Mesostructured TiO_2 prepared from P123; TiO_2^M : Mesostructured TiO_2 prepared from the mixture of P123 and $R^F_8(EO)_9$; TiO_2^F : Mesostructured TiO_2 prepared from $R^F_8(EO)_9$
A_{total} : total activity; A_{HDN} : HDN activity = PB + PCH; A_{HYD} : activity for the hydrogenation route = PCH; A_{DDN} : activity for the direct denitrogenation pathway = PB

Whatever the considered TiO_2-based catalyst, the product distributions are not modified. Considering the mesostructured titania-based catalysts, since after impregnation all the mesostructured titania have a specific surface area in the same range of order, the difference

observed in the catalyst activity (Table 2) cannot be related to the specific surface area effect. In addition, the quantity of the active phase and the promoter rate are the same, therefore the observed modifications cannot be attributed neither to these parameters. Consequently, from Table 2, it can be inferred that the total and the HDN activities can be correlated to the mesopore size of the mesostructured support. Indeed, higher the pore diameter of mesostructured TiO_2 is, higher the activities are. For example the HDN activity of $CoMoS/TiO_2^P$ ($\varnothing \approx 6.6$ nm) is 0.39 $mmol.h^{-1}.g^{-1}$ while the one of $CoMoS/TiO_2^F$ ($\varnothing \approx 2.0$ nm) is 0.14 $mmol.h^{-1}.g^{-1}$, i.e. 2.8 times lower. With a HDN activity of 0.21 $mmol.h^{-1}.g^{-1}$, the catalyst prepared from the dual mesoporous support ($\varnothing \approx 2.0$ nm and 7.7 nm) adopt an intermediate behavior. These results suggest that the large mesopores contribute to the diffusion of the 1234THQ and of the intermediates products inside the channel and facilitate their accessibility to the active phase. The large mesopores can also provide more pathways for products to desorb. A partial pore blocking can occur for the catalyst having the smaller mesopore diameters. If the mesopore size affect the activities, it does not modify the selectivity and the hydrogenated way is by far the predominant route for the denitrogenation of 1234THQ (93% of selectivity). Regarding the conventional $CoMoP/Al_2O_3$ catalyst, the dispersion of the active phase on mesostructured titania supports does not involved a change in the selectivity. The total activity is higher than the one obtained the mesostructured TiO_2-based catalysts (4 $mmol.h^{-1}.g^{-1}$ against 3.1 $mmol.h^{-1}.g^{-1}$ for $CoMoS/TiO_2^P$) but the contribution of HDN is slightly lower (0.3 $mmol.h^{-1}.g^{-1}$ against 0.39 $mmol.h^{-1}.g^{-1}$ for $CoMoS/TiO_2^P$). It can be seen that selectivity towards HYD (88%) is slightly lower than the one obtained with the titania catalyst. The presence of titania thus promote the formation of the nitrogen free products. This can be due to electronic promoter effect, which increase the formation of CUS sites [46]. In addition, in a paper dealing with the effect of TiO_2 addition to alumina support on the hydrodeoxygenation and hydrodenitrogenation activity of the corresponding CoMoS catalyst, Tungkamania et al. have shown that TiO_2 acts as a promoter for the HDN of quinoline, enhancing both the hydrogenation and the C-N bond cleavage [47]. Results obtained here are in good accordance with these observations. The use of CoMoS/M311 and CoMoS/M411 catalysts leads to a lower total activity (2.4 $mmol.h^{-1}.g^{-1}$ against 4.0 and $mmol.h^{-1}.g^{-1}$ for $CoMoP/Al_2O_3$ and $CoMoS/TiO_2^P$). Since they have similar specific surface areas, the difference can be attributed to the absence of intrinsic mesoporosity. Indeed, it should be reminded that for M411 and M311 supports the porosity is interparticular. However, considering the A_{HDN} activity, they behave in a similar way than $CoMoS/TiO_2^P$, showing that the promoter role played by titania is a more crucial parameter than the mesopore size and the type of porosity. Nevertheless, the use of titania supports does not modify the mechanisms involved in the transformation of 1234THQ reported in the literature [9,45,48,49].

The behavior of the mesostructured titania-based catalysts for HDN is different than for HDS. Indeed, when these catalysts are used for the hydrodesulfurization of 46DMDBT the catalytic activity is not affected by the mesopore diameter of the mesostructured TiO_2 support. The total activity is found around 1.64 $mmol.h^{-1}.g^{-1}$. Moreover, a shift towards the direct desulfurization (DDS) selectivity, which is unprecedented in literature, is observed [32]. The direct desulfurization route of 46DMDBT is thus favored in contrary to the conventional CoMoS/alumina catalyst, for which the main pathway of 46DMDBT HDS is the HYD route. These results demonstrate that the amorphous phase involves modifications in the properties of the oxide support material leading to significant changes in the catalytic properties. In addition, thanks to the Brönsted acidity of mesostructured TiO_2 supports, isomerization and dismutation reactions also contribute to the enhancement of the DDS route. By contrast for HDN, the presence of amorphous phase and the Brönsted acidity do not play a significant role in the selectivity and the HYD is the predominant way for HDN of 1234THQ. Even if the

promoter effect of titania has been identified as key parameter for HDN activity, the latter is also affected by the mesopore sizes.

4. Conclusion

Mesostructured TiO_2 having different pore size and kind of porosity (monomodal or dual mesoporosity) with anatase semi crystalline walls have been wet impregnated and sulfided to prepare new catalysts for the hydrodenitrogenation of 1, 2, 3, 4-tetrahydroquinoline. (1234-THQ), used as a model molecule. Results show that due to the promoter effect of titania a slightly higher activity is obtained for the mesostructured TiO_2-based catalyst than for the conventional $CoMoP/Al_2O_3$ one. The hydrogenated route is by far the main way for 1234-THQ HDN. We also demonstrate that the catalytic performance of the mesostructured-titania based catalysts can be correlated to the mesopore sizes.

The use of mesostructured TiO_2 as catalytic support for hydrotreatment is a way to optimize current processes by making them more environmentally efficient. It also demonstrates the great potential of this material to explore other applications.

Credit authorship contribution statement

Sylvette Brunet: Writing - original draft, Supervision, Conceptualization; Teddy Roy: Investigation; Laure Michelin: Investigation; Bénédicte Lebeau: Writing - original draft, Supervision; Jean-Luc Blin: Writing - original draft, Supervision, Conceptualization.

Conflicts of interest

The authors declare that they have no competing interests

Funding

This research received no external funding.

Acknowledgments

Teddy Roy thanks IFP Energies nouvelles for financial support for his master's internship.

References

[1] Air Quality in Europe-2020 report. 2020, European Environmental Agency. Available: https://www.eea.europa.eu//publications/air-quality-in-europe-2020-report. Accessed: 11 January 2024.

[2] H. Carvalho, *J Glob Health* **2019**, *9 (2)*, 020308.

[3] D.S. Jyethi, *Air Quality: Global and Regional Emissions of Particulate Matter, SOx, and NOx*. In Plant Responses to Air Pollution (Eds.: U. Kulshrestha, P. Saxena, P.),. Springer, Singapore, 2016, pp 5-19.

[4] C.D. Koolen, G. Rothenberg, *ChemSusChem* **2019**, *12*, 164-172.

[5] P.R. Robinson, G.E. Dolbear, G.E. (2006). Hydrotreating and Hydrocracking: Fundamentals. In: Practical Advances in Petroleum Processing (Eds.: C.S. Hsu, P.R. Robinson), Springer, New York, 2006, pp 177-218.

[6] F. Bataille, J.L. Lemberton, P. Michaud, G. Pérot, M. Vrinat, M. Lemaire, E. Schulz, M. Breysse, S. Kasztelan, *J. Catal.* **2000**, *191*, 409-422.

[7] R. Prins, In *Handbook of Heterogeneous Catalysis*; Vol. 5 (Eds.: G Ertl, H Knözinger, J Weitkamp); Weinheim, **1997**; p 1908.

[8] M. J. Girgis, B. C. Gates, *Ind. Eng. Chem. Res.* **1991**, *30*, 2021-2058

[9] G. Perot, *Catal. Today* **1991**, *10*, 447-472

[10] J. Ramireza, G. Macıas, L. Cedenoa, A. Gutierrez-Alejandre, R. Cuevasa, P. Castillo, *Catal. Today* **2004**, *98*, 19-30.

[11] A. Stanislaus, A. Marafi, M.S. Rana, *Catal. Today* **2010**, *153*, 1-68.

[12] P. Afanasiev, A. Thiollier, M. Breysse, J.L. Dubois, *Top. Catal.* **1999**, 3-4, 147-160

[13] E. Furimsky, *Stud. Surf. Sci. Catal.* **2007**, 169, 1-387.

[14] S. K. Bej, S. K. Maity, U.T. Turaga, *Energy Fuels* **2004**, 5, 1227-1237.

[15] B. Hinnemann, J.K. Nørdkov, H. Topsøe, *J. Phys. Chem. B* **2005**, 6, 2245-2253.

[16] M. Salimi, A. Tavasoli, L. Rosendahl, Microporous Mesoporous Mater. **2020**, *299*, 110124.

[17] P. Grange, X. Vanhaeren, *Catal. Today* **1997**,*4*, 375-391.

[18] J. Ancheyta, J.G. Speight, *Hydroprocessing of Heavy Oil and Residua*; CRC Press, Taylor and Francis Group: Boca Raton, FL, **2007**.

[19] X. Li, , M. Lu, A. Wang, C. Song, Y. Hu, *J. Phys. Chem. C* **2008**, *112*, 16584-16592.

[20] I. Vázquez-Garrido, A. López-Benítez, G. Berhault, A. Guevara-Lara, *Fuel* **2019**, *236*, 55-64.

[21] J. Ramírez, S. Fuentes, G. Díaz, M. Vrinat, M. Breysse, M. Lacroix, *Appl. Catal.* **1989**, *52*, 211-224.

[22] C. Arrouvel, M. Breysse, H. Toulhoat, P. Raybaud, *J. Catal.* **2005**, *232*, 161-178.

[23] J.C. Morales-Ortuno, R.A. Ortega-Domingueza, P. Hernandez-Hipolito, X. Bokhimi, T.E. Klimova, *Catal. Today* **2016**, *271*, 127-139.

[24] N. Prabhu, A.K. Dalai, J. Adjaye, *Appl. Catal. A Gen.* **2011**, *401*, 1-11.

[25] P. Castillo-Villalón, J. Ramírez, R. Cuevas, P. Vázquez, T. Castañeda, *Catal. Today* **2015**, *259*, 140-149.

[26] H. Wang, X. Cheng *Catal, Surv. Asia* **2015**, *19*, 78-87.

[27] T. Kimura, T., *Chem. Rec.* **2016**, *16*, 445-457.

[28] D.P. Debecker, S. Le Bras, C. Boissière, A. Chaumonnot, C. Sanchez, *Chem. Soc. Rev.* **2018**, *47*, 4112-4155.

[29] K. Zimny, J. Ghanbaja, C. Carteret, M.J. Stébé *New J. Chem.* **2010**, *34*, 2113-2117.

[30] K. Zimny, C. Carteret, M.J. Stébé, J.L. Blin, *J. Phys. Chem. C* **2012**, *116*, 6585-6594.

[31] I. Naboulsi, C. Felipe Linares Aponte, B. Lebeau, S. Brunet, L. Michelin, M. Bonne J.L. Blin, *Chem. Commun.* **2017**, *53*, 2717-2720.

[32] I. Naboulsi, B. Lebeau, C.F. Linares Aponte, S. Brunet, M. Mallet, L. Michelin, M. Bonne, C. Carteret, J.L. Blin, *Appl. Catal. A Gen.* **2018**, *563*, 91-97.
[33] I. Naboulsi, B. Lebeau, L. Michelin, C. Carteret, L. Vidal, M. Bonne, M. Bonne, J.L. Blin, *ACS Appl. Mater. Interfaces* **2017**, *9*, 3113-3122.
[34] J.C Lavalley, R. Anquetil, J. Czyziewska, M. Ziolek, *J. Chem. Soc. Trans.* **1996**, *92* 1263-1266.
[35] M. V. Zakharova, F. Kleitz, F.G. Fontaine, *Dalton Trans.* **2017**, *46*, 3864-3876.
[36] N. Prabhu, A.K. Dalai, J. Adjaye, *Appl. Catal. A Gen.* **2011**, *401*, 1-11.
[37] G. Perot, S. Brunet, C. Canaff, H. Toulhoat, *Bull. Sot. Chim. Belg.* **1987**, *96*, 865-870.
[38] W. F. Zhang, Y. L. He, M. S. Zhang, Z. Yin, Q. Chen, *J. Phys. D: Appl. Phys.* **2000**, *33*, 912-916.
[39] K.S.W. Sing, D.H. Everett, R.A.W. Haul, L. Moscou, R.A. Pierotti, J. Rouquerol, T. Siemieniewska, *IUPAC, Pure Appl. Chem* **1985**, *57*, 603-619.
[40] H. Li, M. Vrinat, G. Berhault, D. Li, H. Nie, P. Afanasiev, *Mater. Res. Bull.* **2013**, *48*, 3374-3382.
[41] T. Roy, J. Rousseau, A. Daudin, G. Pirngruber, B. Lebeau, J.L. Blin, S. Brunet, *Catal. Today* **2021**, *377*, 17-25.
[42] O.Y. Gutiérrez, A. Hrabar, J. Hein, Y. Yu, J. Han, J.A. Lercher, , *J. Catal.* **2012**, *295*, 155-168.
[43] C.N. Satterfield, J.F. Cocchetto, *Ind. Eng. Chem. Proc. Des. Dev.* **1981**, *20*, 53-62.
[44] N. Gnofam, L. Vivier, S. Brunet, J. L. Lemberton, G. Perot, *Catal. Lett.* **1989**, *2*, 81-84.
[45] L. Vivier, V. Dominguez, G. Perot, S. Kasztelan, J. Mol. Catal. **1991**, *61*, 167-275.
[46] W. Huang, H. Liu, M. Huang, Y. Jia, J. Tao, C. Liu, K. Deng, L. Zhao, X. Liu, Q. Wei, Y. Zhou, *Fuel* **2023**, *343*, 127922.
[47] T. Rodseanglung, T. Ratana, M. Phongaksorn, S. Tungkamania, Energy Procedia **2015**, *79*, 378-384.
[48] S. Brunet and G. Perot, React. *Kinet. Catalz Lett.* **1985**, *29*, 15-20.
[49] X. Liu, S. Ding, Q. Wei, Y. Zhou, P. Zhang, Z. Xu, *Fuel* **2021**, *285*, 119039.